Desalination and Water Treatment
www.deswater.com

doi: 10.5004/dwt.2017.11406

64 (2017) 350–358
February

Filtration properties of membranes with active graphene oxide layer

Paulina Cytarska[a], Stanisław Koter[a,*], Grzegorz Trykowski[a], Leszek Stobiński[b]

[a]*Nicolaus Copernicus University in Toruń, Faculty of Chemistry, ul. Gagarina 7, 87-100 Toruń, Poland, Tel. +4856 6114318; email: skoter@umk.pl*
[b]*Warsaw University of Technology, Faculty of Chemical and Process Engineering, ul. Waryńskiego 1, 00-645 Warszawa, Poland*

Received 12 April 2016; Accepted 20 July 2016

ABSTRACT

Filtration properties of membranes obtained by deposition of a few layer graphene oxide onto a polyamide support, with and without borate treatment, were examined. Filtrations of water, dilute solutions of electrolytes (Na_2SO_4, NaCl, $MgSO_4$, $MgCl_2$), and dyes (bromophenol blue, eriochrome black T) were performed. It was found that the observed electrolyte retention series (Na_2SO_4 > NaCl > $MgSO_4$ > $MgCl_2$) was in accordance with the Donnan exclusion theory. The membrane treated with borate and of higher graphene oxide load showed higher retention of sulfates than the untreated one. Despite of lower molecular weight, eriochrome black T was practically completely rejected by both types of membranes, contrary to bromophenol blue, irrespectively of its form (undissociated – retention 68%, dissociated – 85%).

Keywords: Nanofiltration; Graphene oxide; Hydrodynamic permeability; Electrolyte retention; Dye retention

1. Introduction

Nanofiltration (NF) is a membrane filtration technique, which uses membranes of molecular weight cut off (MWCO) between 100 and 1,000 Da [1]. Although a lot of work regarding materials forming active layer has been done [2–4], there is still a need of new materials, which would give a better flow of solvent, sharper MWCO, and better antifouling properties.

In recent years, carbon nanomaterials like nanotubes [5–7], graphene and graphene oxide [8–12] (Fig. 1) as well as graphyne [13] have attracted attention of membranologists. It has been found that (1) water flow through such a material is very fast [14–19], (2) retention properties can be very good [19–22], and (3) addition of such nanomaterials decreases membrane fouling tendency [12,23–25]. Chemical structure of these materials enables their functionalization in a wide range and, consequently, modification of their permeability and retention characteristics. The theoretical papers on how to improve the separation performance of graphene-based membranes have also appeared [6,7,26]. The number of works on new kind of membranes containing graphene oxide (GO, Fig. 1) grows very fast. Among them, one can distinguish membranes with GO layers deposited onto microporous support without any further modification [20,27], crosslinked with a cross-linking agent (e.g., 1,3,5-benzenetricarbonyl trichloride [14], ethylenediamine [22], borate [28]), covalently bound to a support [29], membranes with modified GO [30] or with GO dispersed inside the membrane matrix [25,31–33].

Still, the experimental results exemplifying the electrolyte filtration properties of membrane active layers prepared from GO are rather scarce [20,14,29,22]. As it is described below, these data are not always consistent, probably because of different methods of the active layer preparation.

Han et al. [20] investigated NF membranes obtained by the deposition of base-refluxing reduced graphene oxide on microfiltration membranes (mixed cellulose ester, PVDF and AAO membranes). The thickness of deposited layer varied from 22 to 53 nm. They obtained high retention (>99%) of dyes (methyl blue and direct red 81). The retention of electrolytes (20 mM, transmembrane pressure TMP = 5 bar) was

* Corresponding author.

Presented at the conference on Membranes and Membrane Processes in Environmental Protection (MEMPEP 2016), Zakopane, Poland, 15–19 June 2016.

1944-3994/1944-3986 © 2017 Desalination Publications. All rights reserved.

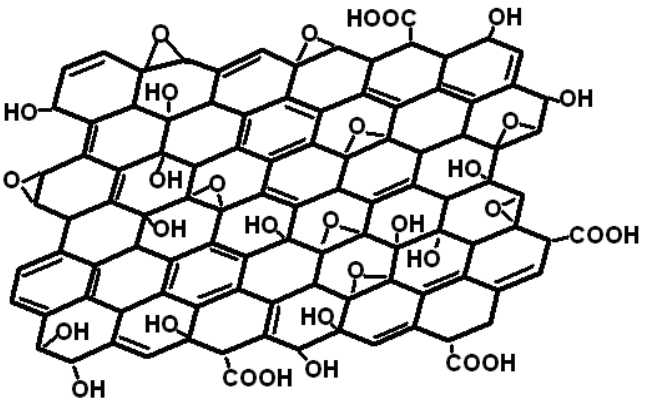

Fig. 1. Graphene oxide (GO) structure.

significantly lower than that of dyes; the observed series of retention –Na_2SO_4 (60%) > NaCl (42%) > $MgSO_4$ (30%) > $MgCl_2$ (20%) – was justified by the Donnan exclusion theory applied to the negatively charged GO layer. According to their data, the expression thickness × (water flux per unit of applied TMP) is more or less constant for the GO thickness ≥ 33 nm, whereas for the thinnest investigated layers 22 and 26 nm, this expression becomes much higher.

Hu and Mi [14] prepared a membrane by the layer-by-layer deposition of GO sheets on a polysulfone support coated with polydopamine. GO sheets were cross-linked with 1,3,5-benzenetricarbonyl trichloride. They found that by covering the membrane support with 5 GO layers, the hydrodynamic permeability of water is reduced by 1 order of magnitude. However, further increase in the number of GO layers (up to 50) did not decrease the water permeability, just the opposite, the permeability doubled (Fig. 5 in [14]). No reasonable explanation of this phenomenon was given. Regarding the electrolyte retention (TMP = 3.4 bar), the retention of Na_2SO_4 (ca. 80%) was higher than that of NaCl (ca. 50%) for 1 mM feed as it could be expected taking into account the Donnan exclusion theory. However, for 10 mM feed, the retention of both electrolytes was practically the same (ca. 30%), which suggested that the concentration of negative charges in the channels was much smaller than one reported in membranes [20].

Wang et al. [29] developed a NF membrane with active layer prepared from O-(carboxymethyl)-chitosan and functionalized with graphene oxide nanosheets. They found a retention of NaCl (17 mM feed) to be 51%–62%, depending on the concentration of GO solution used for the membrane preparation; a retention of Na_2SO_4 using a more diluted feed (7 mM) was much higher – 92%–93%. The observed volume fluxes of pure water and of solutions were non-linear with respect to the applied pressure (TMP = 2.5–15 bar) and the extrapolation to TMP = 0 would yield the flux values much higher than zero. However, no comment on that peculiar effect was given.

Zhang et al. [22], for the membrane made by the GO deposition onto a polydopamine coated polycarbonate support, using the same feed concentrations of NaCl and Na_2SO_4 as Wang et al. [29], obtained substantially lower retention (NaCl – ca. 35%, Na_2SO_4 – ca. 73%). Contrary to the results of Han et al. [20], the retention of $MgSO_4$ (39%) was lower than that of NaCl, although NaCl feed concentration (17 mM) was more than double one of $MgSO_4$ (8.3 mM) and the Donnan exclusion should have been less efficient. The retention of $MgCl_2$ (ca. 33% at 10.5 mM feed) was slightly lower than that of NaCl. The combination of GO with ethylenediamine decreased the fixed charges concentration of the membrane active layer, what resulted in a lower retention of all electrolytes, whereas further treatment with hyperbranched polyethylenimine reversed the sign of fixed charges to positive one, giving the highest retention of salts with divalent cations and monovalent anions (e.g., $MgCl_2$ – ca. 96%), in accordance with Donnan theory.

In this work, we present filtration properties (hydrodynamic permeability, retention) of membranes with a graphene oxide coating as an active layer, deposited onto a polyamide membrane by vacuum filtration. Two kinds of membranes were investigated – with and without borate treatment; till now no work on the filtration through borate crosslinked GO layer has been published. Filtrations of water, dilute solutions of common electrolytes (NaCl, Na_2SO_4, $MgSO_4$, $MgCl_2$), and of two dyes (eriochrome black T, bromophenol blue [BPB]) were examined in experiments carried out with and without stirring.

2. Experimental

A support for GO layer was a membrane made of polyamide-6 formed using phase inversion method. The method and the membrane forming solution are described in [34]. The membrane porosity was determined using Coulter porosimeter. The minimum, maximum and mean flow pore size of the untreated polyamide membrane were 0.24, 0.56, and 0.43 μm, respectively.

The few layer graphene oxide (FL-GO) was obtained by the modified Hummers method [35]. Graphite powder (ACROS) was oxidized by $KMnO_4$ in the presence of concentrated H_2SO_4. The obtained product was purified by distilled water using ceramic membrane, until pH of supernatant reached the value of 5–6. More details are given in [36,37]. Before the FL-GO deposition, 200 mL of distilled water was filtered (vacuum filtration) through the support membrane to remove any residuals after membrane formation. Then, 50 mL of FL-GO suspension (ca. 11 ppm) was filtered in the same manner (the FL-GO load was 260 mg m^{-2}). To strengthen the layer via borate-crosslinking [28], 10 mL of 1 mM $Na_2B_4O_7$ was filtered through the membrane. In this manner, three samples of membrane were prepared, denoted as M1a, M1b, M1c. The fourth one, M2, was prepared without the borate treatment and a more dilute FL-GO suspension (ca. 2.7 ppm) sonicated for 30 min was used (the FL-GO load 66 mg m^{-2}).

2.1. Filtration

The filtration was performed using dead-end SEPA ST cell (Osmonics). The experimental setup is shown in Fig. 2. All experiments were performed at a room temperature (19°C–22°C, the filtration cell was not thermostated; temperature was monitored using an electronic thermometer). The interval of permeate mass reading was 100 s. In the figures showing the time dependence of hydrodynamic permeability, a central moving average (6 points) was applied to avoid an excessive scattering of experimental points.

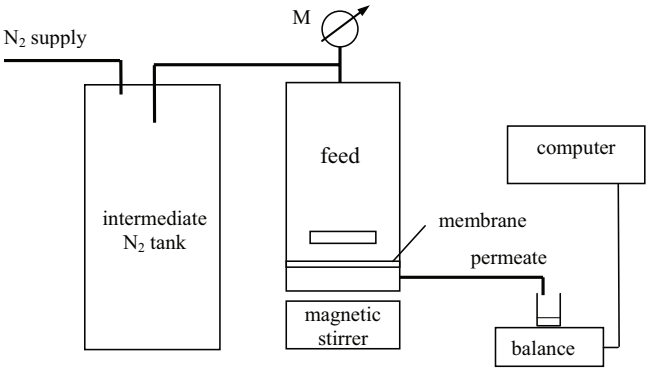

Fig. 2. Experimental setup: M – electronic manometer, T – thermometer.

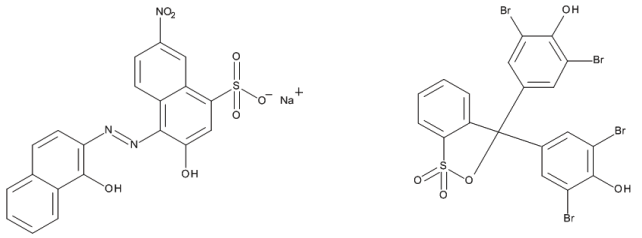

Fig. 3. Structural formula of eriochrome black T (left) and bromophenol blue (right).

As the obtained GO layer was very weak (a finger touch could remove it), we decided to perform the filtrations without stirring before ones with stirring. The filtered substances were: eriochrome black T (M = 461.4 g mol^{-1}, Fig. 3), BPB (M = 670.0 g mol^{-1}, Fig. 3), Na_2SO_4, NaCl, MgSO4, $MgCl_2$.

The retention of dyes was estimated using Eq. (1):

$$R = 1 - A_p / A_f \quad (1)$$

where A is absorbance at the light wavelength giving maximum of A; subscripts p and f denote permeate and feed, respectively. The retention of salts was determined by the conductometric method.

3. Results and discussion

The FL-GO flakes can be characterized as discussed in [36,37]. They show a stack structure with height below 10 monolayers of oxidized graphene. There are numerous oxygen atoms containing moieties such as OH, COOH, C-O-C, C=O and others, which represent more than half of the GO weight. The distance between particular layers of graphite oxide of "diameter" from a few nanometers to a dozen micrometers varies usually from 0.6 to 0.9 nm and is always above 0.4 nm [36,37]. We tried to crosslink the GO flakes using borate as it is described in [12,28]. However, just after the borate treatment, we did not observe any significant improvement of the mechanical stability of deposited layer. The topography image (SEM, the signal SE from the secondary electron detector) of surface membrane layer is shown

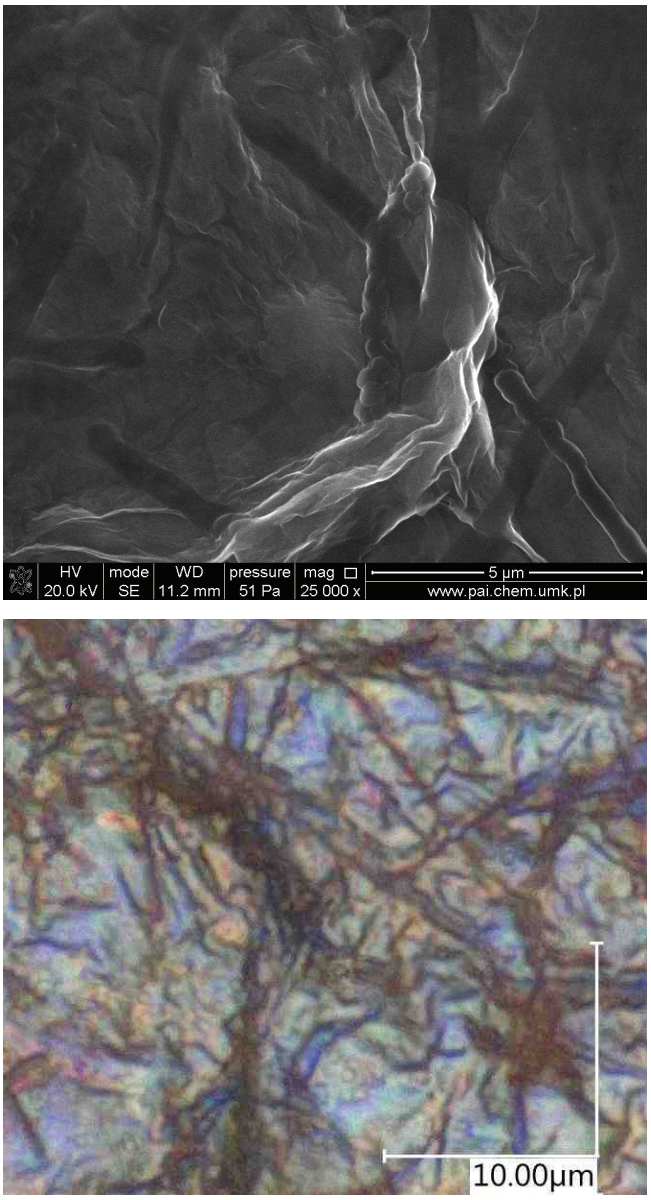

Fig. 4. Membrane sample M1a, FL-GO deposited onto the PA support: (a) SEM (SE detector) topographical image, (b) image from the digital microscope VHX-5000 (Keyence).

in Fig. 4(a). A corrugated, transparent for SEM, layer of GO is visible. The irregularities of the deposited layer can be observed using an optical microscope (Fig. 4(b)).

The transport route through the membrane is shown schematically in Fig. 5. The thick lines represent FL-GO flakes. According to the GO structure (Fig. 1), edges of flakes carry negatively charged carboxylic groups influencing the electrolyte absorption into that active layer. Assuming that the density of FL-GO is ca. two times smaller than that of graphite (the distance between layers is at least twice as that for graphite), the thickness of the deposited FL-GO layer was estimated to be around 0.26 μm (M1) and 0.07 μm (M2). Taking 10 monolayers per flake and their distance 0.9 nm into consideration, the number of flake layers deposited on

the polyamide support was ca. 33 (M1) and 8 (M2). Certainly, the deposited layer could be much thinner; however, the main goal was to check the retention properties. Therefore, we wanted to be sure, that the polyamide support was well covered with graphene oxide.

3.1. Hydrodynamic permeability

To show hydrodynamic permeability changes, the ratio of volume flux, J_v, to pressure difference, Δp, was plotted vs. time. According to the Kedem–Katchalsky theory, the ratio $J_v/\Delta p$ is equal to Eq. (2):

$$L'_p = J_v / \Delta p = L_p(1 - \sigma\Delta\pi / \Delta p) \quad (2)$$

where L_p is hydrodynamic permeability coefficient of solvent, σ is reflection coefficient, Δπ is osmotic pressure difference of solutions separated by the membrane; for enough diluted solutions Δπ is much smaller than Δp and $L'_p \approx L_p$.

The tests with the first sample of membrane (M1a) revealed that J_v of water linearly changed with Δp in the range 5–10 bar with the slope L_p = 0.57 kg m^{-2} h^{-1} bar^{-1} (Fig. 6).

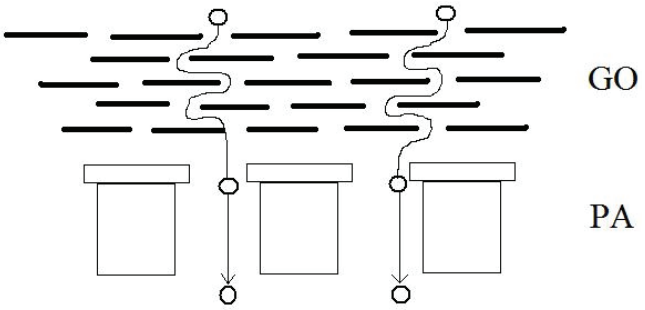

Fig. 5. Transport path of solute molecules through the FL-GO/PA membrane.

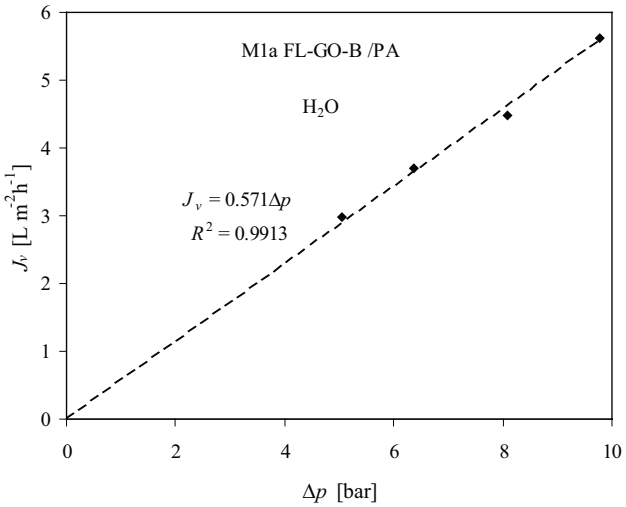

Fig. 6. The dependence of water flux, J_v, through the first sample (M1a) of the FL-GO-B/PA membrane on the transmembrane pressure, Δp.

Increasing Δp to 15 bar, a leakage through the membrane was observed (high increase in L_p) indicating, that the FL-GO flakes of smaller size could slip through support pores of larger size (the mean pore size was 0.43 μm); later we checked that L_p of polyamide support increased ca. 70% when changing Δp from 10 to 15 bar, which could be attributed to the increase in pore sizes. After decreasing Δp to 10 bar, L_p slowly returned to its previous value. L_p for H_2O and the polyamide support was much higher – ca. 20 kg m^{-2} h^{-1} bar^{-1} at 4 bar; during the filtration of 1 mM eriochrome black T, it decreased to 8 kg m^{-2} h^{-1} bar^{-1} still being much higher than the permeability of membranes covered with the FL-GO layer (Figs. 7–9).

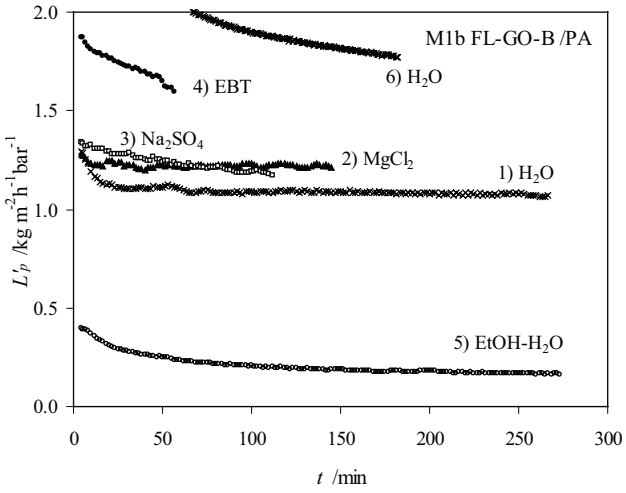

Fig. 7. L'_p obtained in the filtration through the second sample (M1b) of the FL-GO-B/PA membrane (no stirring); EBT – 1 mM eriochrome black T, electrolytes – 1 mM, EtOH-H_2O – 65 vol.%; the runs are numbered; Δp = 10 bar.

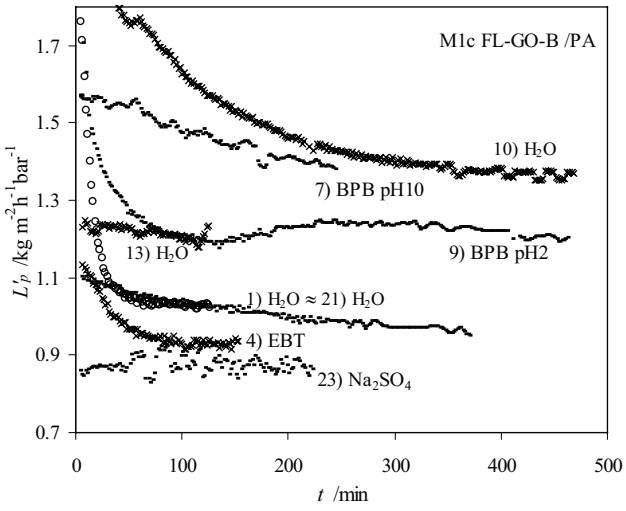

Fig.8. L'_p in the filtration through the third sample (M1c) of the FL-GO-B/PA membrane (no stirring except Na_2SO_4); BPB – 0.2 mM bromophenol blue, EBT – 1 mM eriochrome black T, Na_2SO_4 – 10 mM; Δp = 10 bar.

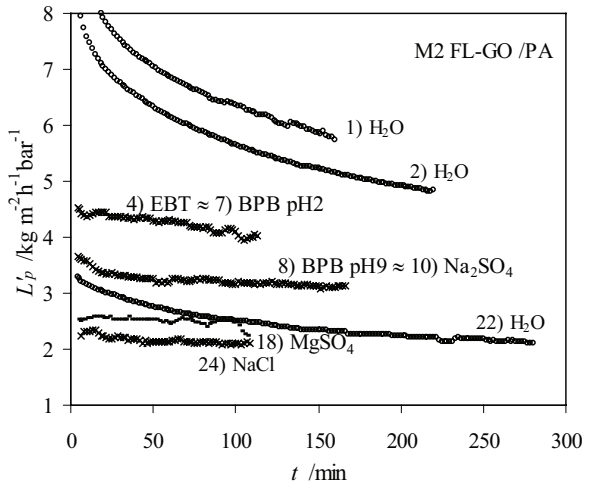

Fig. 9. L'_p in the filtration through the membrane M2 (FL-GO/PA), all runs with stirring except H_2O; BPB – 0.2 mM bromophenol blue, EBT – 1 mM eriochrome black T, electrolytes – 10 mM; Δp = 10 bar.

The permeability coefficient of the second sample of membrane (M1b) for water is shown in Fig. 7. It is seen that compared with the first sample L_p of H_2O (first run), it was ca. two times higher (L_p = 1.1 kg m^{-2} h^{-1} bar^{-1}) indicating that the graphene layer was more leaky. Compared with commercial NF membranes (L_p = 1.5–8.5 kg m^{-2} h^{-1} bar^{-1} [38]) and to ultrathin graphene-NF membrane obtained by Han et al. (L_p = 3.26 L m^{-2} h^{-1} bar^{-1} at the brGO loading 34.0 mg m^{-2} [20]), L_p of our membrane sample was low (L_p = 1.1 at the FL-GO loading 260 mg m^{-2}); however, by reducing the FL-GO load, L_p could be substantially increased (the upper limit was the support permeability).

In the filtration of 1 mM electrolyte solutions (Na_2SO_4, $MgCl_2$, Fig. 7), L'_p was even slightly higher than that for H_2O, and in the case of eriochrome black T (1 mM EBT, fourth run) it increased substantially, however, with decreasing tendency. In the filtration of ethanol-water mixture (65 vol.%, Fig. 6), L'_p decreased ca. six times compared with H_2O. Qualitatively, it was in agreement with the results of Liu et al. [39], who for the mixture ethanol-water (75 wt.%) observed fourfold decrease in permeability compared with pure water (Fig. 1 in [39]). The simplest explanation is that GO prefers more polar molecules (taking relative polarity of H_2O equal 1, for EtOH it is 0.654 [39]). After this run, the filtration of H_2O (sixth run) yielded substantial increase in L_p compared with the first run, again with decreasing tendency.

The first run of water with the third membrane sample (M1c, Fig. 8), obtained in the same manner as M1a and M1b, was initially fast (L_p > 1.7 kg m^{-2} h^{-1} bar^{-1}), then it decreased with time and stabilized at the same level as in the case of M1b (L_p ≈ 1 kg m^{-2} h^{-1} bar^{-1}). Between filtrations of various solutions, the test filtrations of water were also performed. It is seen (Fig. 8), that L_p changed from run to run; at first it increased even above 1.7 (10th run), then decreased to 1.25 kg m^{-2} h^{-1} bar^{-1} (13th run) and in the 21st run it reached practically the same value as in the first run. As expected (Eq. (2)), in the filtration of 10 mM Na_2SO_4 (23rd run, with stirring) L'_p was lower than that of water.

The hydrodynamic permeability of membrane M2 (Fig. 9) prepared from the sonicated FL-GO suspension without borate treatment was substantially higher than that of M1b and M1c. During subsequent filtrations, water permeability decreased reaching the value 2.1 kg m^{-2} h^{-1} bar^{-1} at the end of the 22nd run. This value was only twice as that of the L_p value for the M1c membrane, although for M1c the FL-GO load was four times higher. It means that the hydrodynamic resistance of the polyamide support plays a role and/or the specific hydrodynamic resistance of the FL-GO coating of M1c was lower than that of M2. L_p of M2 was ca. 36% lower than L_p of the membrane from [20] with two times lower GO load (34.0 mg m^{-2}). The decrease in L_p during subsequent filtrations observed for both investigated membranes, M1c and M2, was probably caused by pressing the FL-GO particles into the support pores and/or by the dye adsorption, thus the membrane hydrodynamic resistance increased.

3.2. Retention

In the filtrations without stirring (membrane samples M1b and M1c), eriochrome black T was practically totally rejected. Regarding solutes of incomplete retention, Eq. (3) holds:

$$\frac{R}{R_{\text{int}}} = \frac{1}{R_{\text{int}} + (1 - R_{\text{int}}) \exp(J_v l_p / D_s)} \tag{3}$$

where R_{int} is intrinsic (or real) retention coefficient, calculated from the feed concentration at the membrane surface, l_p is thickness of polarization layer, D_s is diffusion coefficient of solute. According to Eq. (3), the ratio R/R_{int} strongly depends on l_p. We checked that for our data, it was enough to increase l_p to 2–3 mm to reduce R/R_{int} below 0.02. Thus, it was not surprising, that the observed retention of electrolytes was close to zero.

The retention of BPB was determined at pH 2 (undissociated form of BPB) and pH 10 (ionic form of BPB). The results of experiments without stirring are shown in Fig. 10. It is seen, that for pH 2 the initial retention of undissociated BPB was high (R ≈ 0.9), then it decreased to the value ca. 0.1, which was similar to that for the fully dissociated form (pH 10, BPB in the form of divalent anions). The decrease in R with time, observed for BPB in the experiments without stirring, can be qualitatively justified theoretically taking into account the time evolution of the concentration polarization layer. To show this effect, we solved the continuity Eq. (4) for that layer:

$$\frac{\partial c}{\partial t} = -\frac{\partial J_s}{\partial x} \tag{4}$$

where J_s is the solute flux (Eq. (5)):

$$J_s = -D_s \frac{\partial c}{\partial x} + cJ_v \tag{5}$$

with boundary conditions: for x = 0 and $t \geq 0$ $\partial c/\partial x$ = 0, for $x = l_{\text{pol}}$ and $t \geq 0$ $J_s = c_p J_v$ and $c_p = c(l_{\text{pol}}, t)\cdot(1 - R_{\text{int}})$, R_{int} was assumed to be constant, for t = 0 $c(x) = c_{\text{feed}}$. The diffusion coefficient of

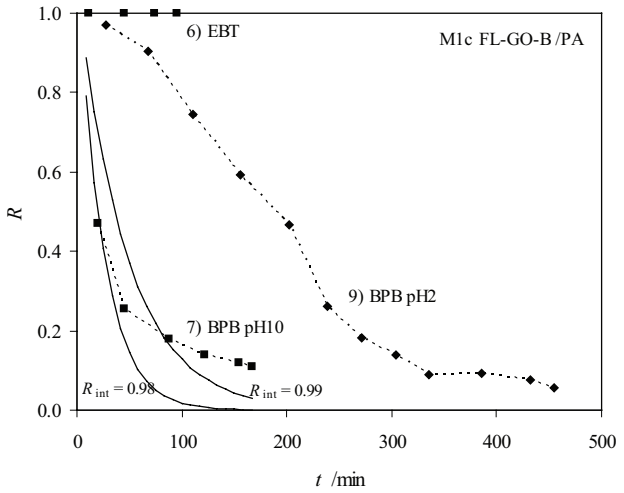

Fig. 10. Retention of eriochrome black T (EBT, 1 mM) and bromophenol blue (BPB, 0.2 mM) at pH 2 and 10 by M1c FL-GO-B/PA membrane; a high value of *R* for BPB at pH 2 was caused by its high adsorption on the polyamide support; filtration without stirring, Δp = 10 bar; solid lines represent theoretical calculations (see the text).

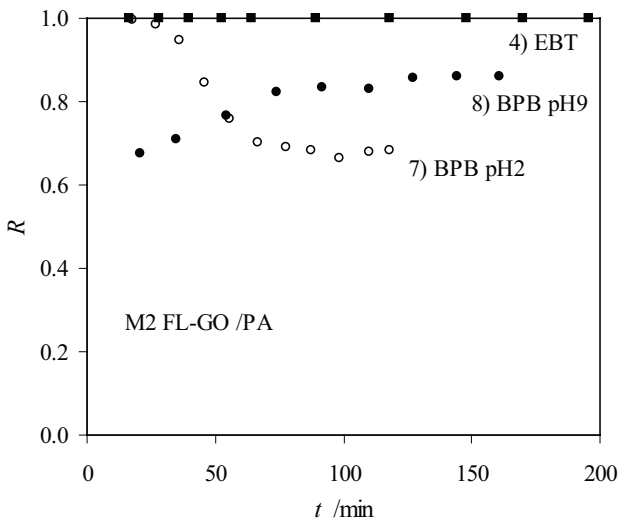

Fig. 11. Retention of eriochrome black T (EBT, 1 mM) and bromophenol blue (BPB, 0.2 mM) at pH 2 and 9 by the M2 FL-GO/PA membrane; a high value of *R* for BPB at pH 2 was caused by its high adsorption on the polyamide support; Δp = 10 bar, the first three points were determined at stirring rate 125 min^{-1}, next ones at 350 min^{-1}.

BPB, $D_s = 0.49 \times 10^{-9}$ m s^{-1}, was estimated using the Wilke–Chang formula [40]. Taking the thickness of the polarization layer, l_{pol}, equal 10 cm and the experimental volume fluxes, we have obtained the decrease in *R* with time as shown by solid lines in Fig. 10, for the assumed values of R_{int} equal 0.98 and 0.99 (BPB, pH10). In fact, R_{int} should decrease, when the solute concentration at the membrane surfaces increases, thus these model lines $R = f(t)$ should be even steeper. Contrary to these model predictions, the decrease in *R* for the run 9) BPB pH2, is delayed. Moreover, these results are also inconsistent with the Donnan exclusion effect, according to which divalent anions of BPB (pH 10) should be more effectively rejected by the negatively charged GO layers (at pH 10 carboxylic groups are dissociated) than univalent anions or undissociated molecules of BPB (pH 2) by the uncharged GO layers (at pH 2 carboxylic groups are undissociated). Thus, the only possible explanation is a high adsorption of BPB on the polyamide support, where at pH 2 amide groups are protonated and monovalents anions of BPB (ca. 9% is present in the solution, as calculated using $pK_{a,1}$ = 3.0 and $pK_{a,2}$ = 4.6 from [41]) can interact with them electrostatically. When the adsorption rate becomes smaller than the BPB permeation rate, then BPB appears in the permeate and *R* decreases. At pH 10, the adsorption is not so high and R decreases much faster. Additional adsorption experiments confirmed that the adsorption of BPB at pH 2 was indeed much higher than that at pH 10.

The experiments with stirring performed on the membrane M2 (no borate treatment) showed (Fig. 11), that the retention of BPB at pH 9 ($R \approx 0.85$) was higher than that at pH 2 ($R \approx 0.68$), according to the expectations. It is seen that at the beginning the retention coefficient of BPB at pH 2 was close to 1, although the stirring rate for the first experimental 3 points was lower (ca. 125 min^{-1}) than for the further part of run (stirring rate ≈ 350 min^{-1}). It clearly indicates that the dye adsorption influenced the observed retention. In the case of BPB at pH 9, *R* increased from the very beginning indicating that the adsorption effect was not so significant and the increase was mainly associated with the increase in the stirring rate.

The retention of eriochrome black T for M2 was very high (>0.999), similarly as for M1b, and was constant during 6 h of filtration. As the additional adsorption experiments showed, the observed high rejection of EBT was not caused by its adsorption on polyamide, but by retention properties of the GO layer.

A lower retention of BPB seems to be strange, when compared with the total rejection of eriochrome black T, which has significantly smaller molecular weight than BPB (461.4 vs. 670.0 g mol^{-1}). The molecular dimensions of both dyes are rather similar – calculated according to chemicalize.org (developed by ChemAxon) minimal and maximal projection areas of the BPB molecule are 0.76 and 0.95 nm^2, respectively, whereas for eriochrome black T which is longer and narrower than BPB – 0.46 and 1.25 nm^2 (Na^+ replaced by H^+), respectively. In that case, the orientation of eriochrome molecule with respect to the membrane pore could be considered as, for example, in [42] where the molecule was treated as cylinder and the effective molecule diameter was calculated (Eq. (4) in [42]) assuming, that the probability distribution of angle between the cylinder axis and the membrane surface, β, was given by cosβ favoring a low angle orientation, which seemed to be a reasonable assumption. However, using that approach, practically no correlation between the retention and the effective molecule diameter was found (Fig. 5 in [42]). To estimate a probable angle of dye molecules on the approach to the GO layer, one should perform theoretical calculations taking into account molecular interactions of all species, which is out of scope of this work. Here we can only

Table 1
Retention of electrolytes by the membranes M1c (borate treatment) and M2 after filtration of dyes

c_f mM^{-1}	Na_2SO_4	NaCl	$MgSO_4$	$MgCl_2$
M1c, stirring rate 125 min^{-1}				
1	0.90	–	0.69	0.18
10	0.87	–	0.58	–
M2, stirring rate 125 min^{-1}				
1	0.86	0.76	0.55	0.21
10	0.46	0.30	0.27	–
M2, stirring rate 350 min^{-1}				
1	0.96	0.81	0.68	0.24
10	0.53	0.33	0.32	–

suggest that a very high rejection of EBT is caused by the parallel orientation of EBT molecule to the membrane surface.

The retention results for electrolytes filtered through the membranes M1c and M2 at two stirring rates are listed in Table 1. As it was mentioned above, without stirring practically no electrolyte retention was observed. It should be noted that filtered dyes may influence the electrolytes filtration because of their adsorption. Therefore, all the data in Table 1 refer to the experiments after dye filtrations.

Analyzing the data in Table 1, one can notice that:

(1) the retention decreased in the order: Na_2SO_4 > NaCl > $MgSO_4$ > $MgCl_2$;
(2) for M1c (with borate), the decrease in R with concentration was not so strong as for M2 (without borate, GO sonificated); for c_f = 1 mM R(M1c) < R(M2), but for c_f = 10 mM R(M1c) > R(M2);
(3) the change of stirring rate from 125 to 350 min^{-1} significantly increased R.

As GO layers are negatively charged, the fixed-charge model [43] can be used for the data interpretation. According to that model, two effects are important – Donnan electrolyte exclusion and mobilities of ions inside membrane's active layer. Using the ideal Donnan equation (Eq. (6)) relating the concentrations of ions outside, c_i, and inside a charged membrane, $\bar{c}_i$:

$$\bar{c}_+\bar{c}_-^{-Z_+/Z_-} = c_+c_-^{-Z_+/Z_-} \tag{6}$$

where z_i is the charge number of ion i; one can find that the concentrations of anions in the negatively charged membrane (at the same salt concentration) are arranged in the following increasing series: Na_2SO_4 < NaCl < $MgSO_4$ < $MgCl_2$. It is in accordance with the decreasing series of retention of these salts. The retention of different salts in terms of the fixed charge model was analyzed in detail by Tsuru et al. [44]. Their results confirmed the retention series Na_2SO_4 > NaCl > $MgCl_2$; unfortunately $MgSO_4$ was not considered there.

Han et al. [20] obtained the same retention series for these electrolytes: Na_2SO_4 – 0.60, NaCl – 0.42, $MgSO_4$ – 0.30, $MgCl_2$ – 0.21 (the values taken from Fig. 6 in [20]). However, for two times more concentrated feed (20 mM), the retention of Na_2SO_4 and NaCl was higher than in our case for 10 mM feed and the M2 membrane. As the volumetric fluxes in their and our filtrations are comparable, another reason could be a lower charge or wider pores of our membrane with substantially thicker GO coating than that of Han's membrane [20].

For the borate treated membrane M1c, the retention of sulfates was higher than that observed for M2 or for the membrane in [20]. It seems, that the treatment of GO with borate anions yields a crosslinked network as shown in Fig. 2 [28] and increases the fixed charge density. This was also confirmed by the smaller decrease in R with the increase in feed concentration comparing with that for M2. However, $MgCl_2$ was rejected by M2 even to lower extent than by M1c. Another factor, which could also be taken into account, is a dependence of the ratio of volume flux to diffusional permeability, J_v/P_s, on the GO load. According to the Spiegler–Kedem equation (Eq. (7)):

$$R_{\text{int}} = \frac{\sigma(1-\exp(-(1-\sigma)J_v/P_s))}{1-\sigma\exp(-(1-\sigma)J_v/P_s)} \tag{7}$$

if the ratio J_v/P_s increases with the GO load at constant σ, then R_{int} also increases.

The retention of Na_2SO_4 from 10 mM feed reported by Hu and Mi [14] ($R \approx 0.3$) was substantially smaller than in our case (R = 0.87 – M1c, 0.53 – M2). This suggests, that their GO layer was less charged. One could think that the crosslinking with 1,3,5-benzenetricarbonyl trichloride decreases the number of carboxylic groups; however, the formation of carboxylic anhydrides, as shown in Fig. 1 [14], seems to be questionable.

It should be mentioned here, that the retention coefficient expressed by Eq. (2) in [20] is just an inconsequent simplification of the expression for the reflection coefficient σ derived by Hoffer and Kedem (Eq. (8)) (Eq. (16) in [43], valid for electrolyte ratio 1:1):

$$\sigma = 1 - \frac{K(K + X/c_s\phi_w}{K + t_1X/c_s\phi_w} \tag{8}$$

where K is the co-ion partition coefficient, X is concentration of fixed charges, ϕ_w is volume fraction of water in the membrane, t_1 is transport number of counterions in free solution, c_s is electrolyte concentration; σ is the upper limit of R_{int} at J_v going to infinity (Eq. (7)). For $c_s >> X$, σ does not become σ = 1 – K, but simply zero (no retention at all), because the Donnan expression for K (derived from Eq. (6)) goes to 1. The result is obvious because in the derivation of Eq. (8), the ion-membrane matrix interactions are neglected [43].

4. Concluding remarks

The filtration properties of membranes with active layer obtained by deposition of the few layer-graphene oxide flakes on a polyamide support were examined. Two types of membrane were investigated – treated and untreated with borate solution, with different loads of graphene oxide.

The hydrodynamic permeability of membranes, at first high, decreased to a certain value during the subsequent filtrations. Two reasons should be taken into account – pressing the FL-GO particles into the support pores and/or the dye adsorption inside the pores, thus, increasing the hydrodynamic membrane resistance.

The membrane treated with borate and of higher GO load showed higher retention of sulfates (Na_2SO_4 – 87%, $MgSO_4$ – 58%) compared with the untreated membrane (Na_2SO_4 – 46%, $MgSO_4$ – 27%, at the same stirring rate and the 10 mM feed) indicating, that borate treatment increased the fixed charge concentration of active layer. However, the positive effect of the higher FL-GO load on the ratio of volume flux to diffusional permeability was not excluded.

The observed order of salt retention by membranes (Na_2SO_4 > NaCl > $MgSO_4$ > $MgCl_2$) was in accordance with the Donnan exclusion theory as applied to the negatively charged membrane. It indicated that ion mobilities inside pores of FL-GO coating were not differentiated too much to disturb the observed sequence.

Regarding examined dyes, eriochrome black T was always almost completely rejected irrespective of the membrane type (R > 0.998). The rejection of BPB of 45% higher molecular weight was substantially lower, as it was shown in experiments, both, with and without stirring. In experiments with stirring, the observed retention of BPB was higher, when it was in the form of divalent anions (pH 9, $R \approx 0.85$) than when it appeared in the undissociated form (pH 2, $R \approx 0.68$). During the dye filtration, one should remember about the dye adsorption on the membrane material, which can lead to the retention overestimation.

The filtration experiments without stirring are helpful in estimating whether the retention of a given solute is complete or not. According to theoretical predictions, even a slight leakage (1%) will cause a substantial decrease in the observed retention coefficient with time. For lower values of the real retention coefficient, the decrease in the observed one can be so fast, that no solute retention will be observed.

References

[1] A.B. Kołtuniewicz, E. Drioli, Membranes in Clean Technologies, Theory and Practice, Vol. 1, Wiley-VCH Verlag GmbH & Co. KGaA, Weinheim, 2008.

[2] R.J. Petersen, Composite reverse osmosis and nanofiltration membranes (review), J. Membr. Sci., 83 (1993) 81–150.

[3] B. Van der Bruggen, Chemical modification of polyethersulfone nanofiltration membranes: a review, J. Appl. Polym. Sci., 114 (2009) 630–642.

[4] L.Y. Ng, A.W. Mohammad, C.Y. Ng, A review on nanofiltration membrane fabrication and modification using polyelectrolytes: effective ways to develop membrane selective barriers and rejection capability, Adv. Colloid Interface Sci., 197 (2013) 85–107.

[5] B. Zhao, Z. Lei, W. Xian-ying, J. Yang, T. Zhi-hong, Y. Guang-zhi, Q. Han-xun, H. Xing, Research progress in nanofiltration membrane based on carbon nanotubes, New Carbon Mater., 26 (2011) 321–327.

[6] M. Thomas, B. Corry, A computational assessment of the permeability and salt rejection of carbon nanotube membranes and their application to water desalination, Phil. Trans. R. Soc. A, 374 (2016) 20150020; http://dx.doi.org/10.1098/rsta.2015.0020.

[7] M.E. Suk, N.R. Aluru, Water transport through ultrathin graphene, J. Phys. Chem. Lett., 1 (2010) 1590–1594.

[8] D. Cohen-Tanugi, J.C. Grossman, Water desalination across nanoporous graphene, Nano Lett., 12 (2012) 3602–3608.

[9] A. Aghigh, V. Alizadeh, H.Y. Wong, M.S. Islam, N. Amin, M. Zaman, Recent advances in utilization of graphene for filtration and desalination of water: a review, Desalination, 365 (2015) 389–397.

[10] H.M. Hegab, L.D. Zou, Graphene oxide-assisted membranes: fabrication and potential applications in desalination and water purification, J. Membr. Sci., 484 (2015) 95–106.

[11] G.P. Liu, W.Q. Jin, N.P. Xu, Graphene-based membranes, Chem. Soc. Rev., 44 (2015) 5016–5030.

[12] K.A. Mahmoud, B. Mansoor, A. Mansour, M. Khraisheh, Functional graphene nanosheets: the next generation membranes for water desalination, Desalination, 356 (2015) 208–225.

[13] J.L. Kou, X.Y. Zhou, Y.X. Chen, H.J. Lu, F.M. Wu, J.T. Fan, Water permeation through single-layer graphyne membrane, J. Chem. Phys., 139 (2013) 064705.

[14] M. Hu, B.X. Mi, Enabling graphene oxide nanosheets as water separation membranes, Environ. Sci. Technol., 47 (2013) 3715–3723.

[15] J.A. Prince, S. Bhuvana, V. Anbharasi, N. Ayyanar, K.V.K. Boodhoo, G. Singh, Ultra-wetting graphene-based membrane, J. Membr. Sci., 500 (2016) 76–85.

[16] N. Wei, X.S. Peng, Z.P. Xu, Understanding water permeation in graphene oxide membranes, ACS Appl. Mater. Interf., 6 (2014) 5877–5883.

[17] B. Liu, R. Wu, J.A. Baimova, H. Wu, A.W. Law, S.V. Dmitriev, K. Zhou, Molecular dynamics study of pressure-driven water transport through graphene bilayers, Phys. Chem. Chem. Phys., 18 (2016) 1886–1896.

[18] J. Wang, P. Zhang, B. Liang, Y. Liu, T. Xu, L. Wang, B. Cao, and K. Pan, Graphene oxide as an effective barrier on a porous nanofibrous membrane for water treatment, ACS Appl. Mater. Interfaces, 8 (2016) 6211–6218.

[19] Y. Han, Y. Jiang, C. Gao, High-flux graphene oxide nanofiltration membrane intercalated by carbon nanotubes, ACS Appl. Mater. Interf., 7 (2015) 8147–8155.

[20] Y. Han, Z. Xu, C. Gao, Ultrathin graphene nanofiltration membrane for water purification, Adv. Functional Mater., 23 (2013) 3693–3700.

[21] S.J. Gao, H.L. Qin, P.P. Liu, J. Jin, SWCNT-intercalated GO ultrathin films for ultrafast separation of molecules, J. Mater. Chem. A, 3 (2015) 6649–6654.

[22] Y. Zhang, S. Zhang, T.S. Chung, Nanometric graphene oxide framework membranes with enhanced heavy metal removal via nanofiltration, Environ. Sci. Technol., 49 (2015) 10235–10242.

[23] Y. Mansourpanah, H. Shahebrahimi, E. Kolvari, PEG-modified GO nanosheets, a desired additive to increase the rejection and antifouling characteristics of polyamide thin layer membranes, Chem. Eng. Res. Des., 104 (2015) 530–540.

[24] H.Y. Liu, G.Q. Zhang, C.Q. Zhao, J.D. Liu, F.L. Yang, Hydraulic power and electric field combined antifouling effect of a novel conductive poly(aminoanthraquinone)/reduced graphene oxide nanohybrid blended PVDF ultrafiltration membrane, J. Mater. Chem. A, 3 (2015) 20277–20287.

[25] S. Bano, A. Mahmood, S.J. Kim, K.H. Lee, Graphene oxide modified polyamide nanofiltration membrane with improved flux and antifouling properties, J. Mater. Chem. A, 3 (2015) 2065–2071.

[26] H.B. Huang, Y.L. Ying, X.S. Peng, Graphene oxide nanosheet: an emerging star material for novel separation membranes, J. Mater. Chem. A, 2 (2014) 13772–13782.

[27] J.J. Song, Y. Huang, S.-W. Nam, M. Yu, J. Heo, N. Her, J.R.V. Flora, Y. Yoon, Ultrathin graphene oxide membranes for the removal of humic acid, Sep. Purif. Technol., 144 (2015) 162–167.

[28] Z. An, O.C. Compton, K.W. Putz, L.C. Brinson, S.T. Nguyen, Bio-inspired borate cross-linking in ultra-stiff grapheme oxide thin films, Adv. Mater., 23 (2011) 3842–3846.

[29] J. Wang, X. Gao, J. Wang, Y. Wei, Z. Li, C. Gao, O-(carboxymethyl)-chitosan nanofiltration membrane surface functionalized with graphene oxide nanosheets for enhanced desalting properties, ACS Appl. Mater. Interf., 7 (2015) 4381–4389.

[30] N. Wang, S. Ji, G. Zhang, J. Li, L. Wang, Self-assembly of graphene oxide and polyelectrolyte complex nanohybrid membranes for nanofiltration and pervaporation, Chem. Eng. J., 213 (2012) 318–329.

[31] B.M. Ganesh, A.M. Isloor, A.F. Ismail, Enhanced hydrophilicity and salt rejection study of graphene oxide-polysulfone mixed matrix membrane, Desalination, 313 (2013) 199–207.
[32] S.A. Zinadini, A.A. Zinatizadeh, M. Rahimi, V. Vatanpour, H. Zangeneh, Preparation of a novel antifouling mixed matrix PES membrane by embedding graphene oxide nanoplates, J. Membr. Sci., 453 (2014) 292–301.
[33] M. Safarpour, A. Khataee, V. Vatanpour, Thin film nanocomposite reverse osmosis membrane modified by reduced graphene oxide/TiO2 with improved desalination performance, J. Membr. Sci., 489 (2015) 43–54.
[34] P. Adamczak, Formation of Membranes from Polyamide-6 by the Phase Inversion Method, A. Narębska (Ed.), Membranes and Membrane Separation Techniques (in Polish), Wydawnictwo UMK, Toruń, 1996.
[35] W.S. Hummers, R.E. Offeman, Preparation of graphitic oxide, J. Am. Chem. Soc., 80 (1958) 1339–1339.
[36] B. Lesiak, L. Stobinski, A. Małolepszy, M. Mazurkiewicz, L. Kövér, J. Tóth, Preparation of graphene oxide and characterization using electron spectroscopy, J. Electron Spectrosc. Relat. Phenom., 193 (2014) 92–99.
[37] L. Stobinski, B. Lesiak, A. Malolepszy, M. Mazurkiewicz, B. Mierzwa, J. Zemek, P. Jiricek, I. Bieloshapka, Graphene oxide and reduced graphene oxide studied by the XRD, TEM and electron spectroscopy methods, J. Electron Spectrosc. Relat. Phenom., 195 (2014) 145–154.
[38] S. Koter, Determination of the parameters of the Spiegler–Kedem–Katchalsky model for nanofiltration of single electrolyte solutions, Desalination, 198 (2006) 335–345.
[39] R. Liu, G. Arabale, J. Kim, K. Sun, Y. Lee, C. Ryu, C. Lee, Graphene oxide membrane for liquid phase organic molecular separation, Carbon, 77 (2014) 933–938.
[40] R.K. Sinnott, Coulson and Richardson's Chemical Engineering, vol. 6: Chemical Engineering Design, 3rd ed., Butterworth-Heinemann, 1999.
[41] J. Ferreira, E.M. Girotto, pH Effects on the ohmic properties of bromophenol blue-doped polypyrrole film, J. Braz. Chem. Soc., 21 (2010) 312–318.
[42] L. Braeken, R. Ramaekers, Y. Zhang, G. Maes, B. Van der Bruggen, C. Vandecasteele, Influence of hydrophobicity on retention in nanofiltration of aqueous solutions containing organic compounds, J. Membr. Sci., 252 (2005) 195–203.
[43] E. Hoffer, O. Kedem, Hyperfiltration in charged membranes: the fixed charge model, Desalination, 2 (1967) 25–39.
[44] T. Tsuru, S.-I. Nakao, S. Kimura, Calculation of ion rejection by extended Nemst-Planck equation with charged reverse osmosis membranes for single and mixed electrolyte solutions, J. Chem. Eng. Jpn., 24 (1991) 511–517.